Published in final edited form as:
Proteomics. 2014 October ; 14(19): 2156–2166. doi:10.1002/pmic.201400092.

Probing phosphorylation-dependent protein interactions within functional domains of histone deacetylase 5 (HDAC5)

Amanda J. Guise, **Rommel A. Mathias**, **Elizabeth A. Rowland**, **Fang Yu**, and **Ileana M. Cristea***
Princeton University, Department of Molecular Biology, Princeton, NJ 08544

Abstract

Class IIa histone deacetylases (HDACs) are critical transcriptional regulators, shuttling between nuclear and cytoplasmic cellular compartments. Within the nucleus, these HDACs repress transcription as components of multi-protein complexes, such as the nuclear co-repressor (NCoR) and beclin-6 co-repressor (BCoR) complexes. Cytoplasmic relocalization releases this transcriptional repressive function. Class IIa HDAC shuttling is controlled, in part, by phosphorylations flanking the nuclear localization signal (NLS). Furthermore, we have reported that phosphorylation within the NLS by the kinase Aurora B modulates the localization and function of the class IIa HDAC5 during mitosis. While we identified numerous additional HDAC5 phosphorylations, their regulatory functions remain unknown. Here we studied phosphorylation sites within functional HDAC5 domains, including the deacetylation domain (DAC, Ser755), nuclear export signal (NES, S1108), and an acidic domain (AD, Ser611). We have generated phosphomutant cell lines to investigate how absence of phosphorylation at these sites impacts HDAC5 localization, enzymatic activity, and protein interactions. Combining molecular biology and quantitative mass spectrometry, we have defined the interactions and HDAC5-containing complexes mediated by site-specific phosphorylation and quantified selected changes using parallel reaction monitoring (PRM). These results expand the current understanding regarding HDAC regulation, and the functions of this critical family of proteins within human cells.

Keywords

class IIa HDAC; histone deacetylase 5; HDAC3; MEF2D; phosphorylation

1. Introduction

The eleven human histone deacetylases (HDACs) are essential transcriptional regulators with critical roles in development, epigenetic response to diverse stimuli, and host response to disease progression[1–6]. HDAC dysfunction is linked to the progression of both cancer and viral infection[6–8]. Thus, HDACs are promising targets for the development of anti-cancer and antiviral therapeutics. Indeed, the HDAC inhibitor SAHA is currently approved for treatment of T-cell lymphomas. HDAC inhibition has also been shown to promote

*Corresponding author: Ileana M. Cristea, 210 Lewis Thomas Laboratory, Department of Molecular Biology, Princeton University, Princeton, NJ 08544, Tel: 6092589417, Fax: 6092584575, icristea@princeton.edu.

The authors declare no financial or commercial conflicts of interest.

reactivation of latent cellular reservoirs of HIV-1 both in cell culture and in primary CD4+ T-cells isolated from HIV-1 positive patients[9], as well as reactivation of dormant herpes simplex virus 1 (HSV-1) and human cytomegalovirus (HCMV)[7, 10]. Thus, defining the mechanisms involved in HDAC regulation is critical to understanding their contribution to human disease progression.

The HDAC family is subdivided into four classes based on sequence similarity and structural homology: class I (HDAC1, 2, 3, and 8); class IIa (HDAC4, 5, 7, and 9); class IIb (HDAC6 and 10); and class IV (HDAC 11). Along with their class I counterparts, the class IIa HDACs (HDAC4, 5, 7, and 9) act to repress transcription of downstream gene targets through deacetylation of lysine residues at target promoter regions. Lysine deacetylation is thought to promote adoption of a more compact, closed chromatin conformation, which in turn limits the ability of transcription factors and additional components of the nuclear transcriptional machinery to access the DNA template. Class IIa HDACs act as components of multi-protein complexes, including the nuclear corepressor (NCoR) and the bcl-6 corepressor (BCoR) complexes to carry out their repressive functions[11–14]. These functions are critical to epigenetic response to drug stimulus, as well as in cardiac development[3, 15, 16]. Class IIa HDACs share a common domain structure, including a C-terminal nuclear export sequence (NES), deacetylation domain (DAC), acidic domain (AD), nuclear localization signal (NLS), and an N-terminal extension containing transcription factor binding domains (MEF) (Figure 1A)[17, 18]. Class IIa HDACs are further characterized by a dual-compartment localization, which is achieved through a phosphorylation-dependent mechanism of nucleo-cytoplasmic shuttling[8, 19–22]. In the case of HDAC5, phosphorylation of two serine residues (Ser259 and Ser498) flanking the NLS promote the binding of 14–3–3 chaperone proteins, which escort HDAC5 to the cytoplasm[23]. HDAC5 is thus spatially removed from its nuclear targets, relieving HDAC-induced transcriptional repression. The roles of HDAC5 within the cytoplasm are less well understood; however, histone deacetylases evolutionarily predate histones, indicating that HDAC5 likely has additional cytoplasmic and nuclear substrates[24]. Cytoplasmic activity of HDACs is not unprecedented, as the predominately cytoplasmic enzyme HDAC6 has been shown to deacetylate tubulin[25]. Nuclear import of HDAC5 is achieved, in part, through the dephosphorylation of Ser259 and Ser498 by cytoplasmic phosphatases, and, as we previously reported, aided by the phosphorylation of Ser279 within the NLS[26]. Ser279 has been shown to be phosphorylated by protein kinase A (PKA) in Cos7 cells and cardiomyocytes[27] and by cyclin-dependent kinase 5 (Cdk5) in neurons [28], indicating that phosphorylation may be an important mechanism of tissue-specific HDAC regulation. Furthermore, we found a mitotic phosphorylation of the adjacent NLS residue Ser278 by the kinase Aurora B, providing evidence of additional roles for HDAC5 during specific stages of the cell cycle[29]. Ser278 phosphorylation was accompanied by sequestration of a pool of HDAC5 within a phosphorylation gradient at the mitotic midzone[29]. It is possible that this phosphorylation promotes midzone localization of class IIa HDACs to protect re-forming daughter nuclei from chromatin remodeling during nuclear division. Importantly, our previous observation thatHDAC5 is phosphorylated at 17 distinct residues (Figure 1A) points to a broad role for phosphorylation in the dynamic regulation of protein functions.

Having previously examined both phosphorylation sites within the NLS, here we investigate the additional HDAC5 phosphorylations within its functional domains. We have generated a series of HDAC5 phosphomutants (Ser to Ala) to assess the role of phosphorylation within the AD, DAC, and NES domains. Our investigation demonstrated that these sites are well conserved within HDAC5 mammalian orthologues, while being specific for HDAC5 within the class IIa enzyme family. Furthermore, mass spectrometry analyses have indicated that S611 within the AD and S1108 within the NES are prominently phosphorylated. Using microscopy and enzymatic assays, we determined the impact on protein localization and deacetylation activity. Next, we examined changes in HDAC5 protein interactions upon mutation of individual phosphorylation sites. We observed changes in associations with transcription factors and components of the NCoR complex, which we further validated by Western blotting and targeted MS/MS approaches using parallel reaction monitoring (PRM). Overall, these results expand the current understanding regarding the regulation of HDAC function via dynamic site-specific phosphorylation.

2. Materials and Methods

Cell Line Construction

HDAC5- and EGFP-expressing HEK293 cell lines were generated as previously described [26]. Briefly, HEK293 cells lines expressing EGFP, HDAC5-EGFP, or Ser-to-Ala phosphomutant forms of HDAC5 (S611A, S755A, S1108A) were constructed using retroviral transduction (Phoenix™ retrovirus expression system, Orbigen). Phosphorylation site mutations were generated from the wild-type HDAC5 construct through site-directed mutagenesis with appropriate primers (Supplemental Table S1), and EGFP was obtained from pEGFP-N1 (Clontech). Selection for cells expressing the target proteins was achieved through treatment of cultures with genetic in (300 mg/L) prior to Fluorescence Activated Cell Sorting (Vantage S.E. with Turbosort II, Becton Dickinson).

Immunoaffinity Purification of HDACs

Immunoaffinity purifications of HDAC5, phosphomutants, or GFP control were performed using approaches that we previously described for mammalian HDACs[14]. The resulting cell lines were cultured in DMEM (Life Technologies) supplemented with 10% fetal bovine serum and 1% Pen/Strep (both from Gemini MedSupply) using mammalian cell culture procedures until confluence. Cells were harvested by trypsinization followed by centrifugation. Cell pellets were washed with twice with 50 mL sterile Dulbecco's phosphate buffered saline (DPBS) (Life Technologies) to fully remove media traces. The cell pellet was then resuspended in a freezing buffer containing HEPES, polyvinylpyrrolidone, and a protease inhibitor cocktail (Sigma) and frozen, as previously described[30]. Frozen cell pellets were ground into cell powder through cryogenic lysis using a Retsch MM301 Mixer Mill. Cell powder from 10 confluent plates (ca. 0.80 g) of HDAC5-EGFP or EGFP (control) cells was homogenized in 10 mL of ice-cold optimized lysis buffer (20 mM HEPES-KOH, pH = 7.4; 0.1 M potassium acetate; 2 mM $MgCl_2$; 0.1% Tween-20; 1 μM $ZnCl_2$; 1 μM $CaCl_2$; 0.5% Triton X-100; 250 mM NaCl; 4 1 μg/mL DNase I; 1/100 (v/v) protease and phosphatase inhibitor cocktails) and disrupted by Polytron (Kinematica). Resulting cell lysates were then centrifuged at 8000 x g for 10 minutes to

pellet the insoluble cell material. Immunoisolation of EGFP-tagged protein was performed by incubating M-270 magnetic beads (Life Technologies) conjugated with in-house-generated anti-GFP antibodies (rabbit, polyclonal) with cell lysate supernatants for 60 minutes at 4° C with rotation. 10 mg of antibody-conjugated beads were used per 10 mL of lysate. Following isolation, beads were washed four times with modified lysis buffer (no DNase I, protease inhibitors, or phosphatase inhibitors) and twice with PBS prior to elution of immunoisolates from beads in 1X LDS NuPAGE Sample Buffer (Life Technologies).

Mass-spectrometry, Proteomic Analysis, and Construction of Protein Networks

Immunoisolates were separated by 1D-PAGE prior to analysis by mass spectrometry as previously described[29]. Samples were heated in the presence of reducing agent (Life Technologies) and treated with iodoacetamide prior to gel electrophoresis using a 4–12% Bis-Tris precast PAGE system (Life Technologies). The entire gel lane was excised and sliced into 1 mm pieces using a gel slicer (Brinkmann), which were then loaded into individual wells in 96-well plates and destained in a 50% ammonium bicarbonate (ABC) and 50% acetonitrile (ACN) solution for 2 × 10 min at 4 °C with agitation. Gel pieces were then dehydrated with ACN and rehydrated with 50 mM ABC. Following a final dehydration in ACN, gel pieces were digested in-gel with 5 ng/μL trypsin in ABC for 8 hours. Digestions were quenched with 1% formic acid (FA) and extracted at RT. Samples were concentrated to 25–50 μL using vacuum centrifugation and desalted using StageTips[31] with an Empor C18 filter (3M).

Peptides were analyzed by nLC-MS/MS using reverse phase liquid chromatography (Dionex Ultimate 3000 RSLC) coupled to mass spectrometry analysis on an LTQ Orbitrap Velos with ETD instrument (ThermoFisher Scientific). Peptide separation was achieved over an Acclaim PepMap RSLC column (1.8 μm, 75 μm × 25 cm) with a 90 minute gradient (flow rate = 250 nL/min). Mass spectra were acquired with the instrument operating in the data-dependent mode (no preview scan, AGC enabled). The top 20 most intense ions were isolated for CID fragmentation in the linear ion trap following full-scan (m/z = 350–1700 Da) acquisition in the Orbitrap mass analyzer (r = 30000 for m/z = 400). Target ion intensity values were set for full scan FTMS (at 1E6) and fragment ion $ITMS^2$ (at 3E5) and injection times were limited to 300 ms and 100 ms, respectively. A 2.0 Th isolation window was selected for CID fragmentation (normalized collision energy = 30, activation time = 10 ms).

Following acquisition, MS^2 spectra were extracted, filtered, and searched against a sequence database generated from human protein sequences (21570 total entries) (UniProt-SwissProt, 2010–11) using Proteome Discoverer (PD1.4) with SEQUEST (ThermoFisher Scientific). Common contaminants were manually included within this database. Entries were reversed and concatenated to forward sequences and were then added to the database in order to serve as decoy hits for the estimation of false discovery rates, as previously reported[32]. The LTQ Orbitrap Velos was operated using lock mass to limit mass errors to <2 ppm[33], and spectrum searching allowed a tolerance of two missed cleavages and a precursor mass errors search window ≤ 10 ppm. Fragment mass tolerance was set at 0.5 Da. These searches also included static modification of cysteine (carbamidomethylation, +57 Da) and variable modification of methionine (oxidation, +16), serine/threonine/tyrosine (phosphorylation,

+80 Da), and lysine (acetylation, +42 Da). PD1.4/SEQUEST results were further analyzed and processed using Scaffold 4 (Proteome Software) incorporating an X!Tandem (Beavis Informatics) search. Spectral match probabilities relied on calculations from PeptideProphet [34] in Scaffold 4 and Percolator [35] in PD1.4. Percolator filtering based on q-values allowed the global FDR to be limited to ≤ 1%.

Protein identifications were subsequently filtered using the SAINT algorithm [36] to determine specificity. A stringent probability score of >0.90 was selected as a specificity cut-off. After SAINT filtering, 94 proteins were considered likely specific interactions of HDAC5. Due to the shuttling nature of class IIa HDACs, five established HDAC protein interactions with SAINT scores not passing the p>0.90 filter were manually added to the protein lists (MEF2C, MEF2D, AURB, CAMK2D, $PP2A_{cs}$). Label free relative quantitation using spectral counting was then performed for the combined list of proteins. Spectrum counts for individual proteins were normalized to the HDAC5 bait counts as well as to prey protein lengths. Fold changes were calculated using the average counts from each phosphomutant (n=3) compared to wild-type HDAC5 (n=3). Protein abundance ratios were mapped to interaction networks constructed using the STRING database[37] and were visualized using Cytoscape [38].

Parallel Reaction Monitoring (PRM) Analysis of Protein Interactions

A list of target peptides including amino acid sequence and charge state information for individual interacting proteins was compiled for targeted parallel reaction monitoring by LC-MS/MS. Target peptides were loaded into Skyline to allow selection of candidate fragment ions. MS acquisition methods were modified in XCalibur as follows: BeginPos = 15; EndPos = 110; Collision Engery = 35; Peptide Note = Precursor Mass + 25. Following data-independent acquisition,. raw files were imported into Skyline[39]. XICs were manually inspected and filtered to confirm peptide/protein identities. Peak areas were quantified from at least two transitions per peptide and areas were normalized to HDAC5 peak areas (n=2 peptides).

Phosphopeptide Quantitation

Phosphopeptide quantitation was carried out using Skyline[39]. Proteome Discoverer-generated. msf files were loaded into Skyline to build a spectral library for HDAC5 peptides with an applied peptide cut-off score of 0.8 to select for high quality spectra. Raw MS data files were then imported into Skyline and phosphorylated (MOD) and non-phosphorylated (UNMOD) peptide target peaks were identified at matched to peptide retention times. Peak areas (PA) were determined for individual peptides and PA ratios were calculated as $PA_{MOD}/(PA_{MOD}+PA_{UNMOD})$ to estimate the percentage of HDAC5 phosphorylated at individual sites Phosphorylation estimates were based on ratios determined in n=4 replicates. The peptides containing the phosphorylations at the AD and DAC sites were detected in all four experiments. However, the C-terminal peptide of HDAC5, containing the NES site, was more difficult to detect as either unmodified or modified form (i.e., neither the unmodified nor the modified forms were detected in two of the replicate experiments). Nevertheless, this part of the protein was reproducibly detected as both unmodified and modified forms in n=2 replicates, which were used to estimate the phosphorylation levels.

Given the difficulty in sequencing this part of the protein, we chose to represent these as ranges of possible phosphorylation levels at each site.

Immunofluorescence Microscopy

HEK293 cells expressing phosphomutant HDAC5-EGFP, wild-type HDAC5-EGFP, or EGFP alone were grown to 80% confluence on glass coverslips in normal media. Cells were then washed with DPBS (Life Technologies) and fixed with 2% Paraformaldehyde for 15 min. Following a 0.1 mM glycine/DPBS wash, cells were permeabilized with 0.1% Triton X-100/DPBS for 15 min and blocked overnight in blocking buffer (2% bovine serum albumin (BSA); 0.2% Tween-20 in DPBS). The blocked cells were then incubated with primary anti-GFP antibodies (in-house generated) for 60 min at room temperature (RT) in blocking buffer. Cells were washed with 0.2% Tween/DPBS and incubated with mouse anti-rabbit Alexa488 fluorescent antibodies (Life Technologies) in blocking solution for 60 min at RT. DAPI (4′,6-diamidino-2-phenylindole) staining was carried out at RT for 30 minutes (1 μg/mL in DPBS), and coverslips were mounted on slides with Aqua-Poly/Mount mounting media (Polysciences) prior to visualization using a Nikon A1 confocal microscope an 100x oil immersion lens.

Immunoblotting and Validation of Protein Interactions

Selected HDAC interactions were validated using standard Western blotting techniques. Briefly, HDACs and interacting proteins were isolated using immunoaffinity purification with magnetic beads as described in this manuscript. Immunoisolates were separated by SDS-PAGE and proteins were transferred to a PVDF (polyvinylidene fluoride) membrane for the purposes of immunoblotting. Membranes were incubated with primary antibodies, washed, and incubated with HRP-conjugated secondary antibodies (Sigma-Aldrich, Roche). Protein detection was carried out using ECL or ECL Prime Detection Reagents (Amersham).

Protein Structure Prediction

Structural model prediction for HDAC5 was performed using the I-TASSER server [40–42]. Fold regions are assigned using sequence similarity to solved protein structures within the RCSB PDB (Research Collaboratory for Structural Bioinformatics Protein Data Bank) library. Individual fold regions are assembled by the server into a full-length protein model using Monte Carlo simulations, followed by re-assembly based on centroid clustering. The most prominent PDB structures used as templates for I-TASSER structural prediction of HDAC5 were partial structures of HDAC4, HDAC7, and HDAC1.

3. Results and Discussion

Prominent functional domain phosphorylation at sites specific to HDAC5 within the class IIa enzyme family

We have recently reported that HDAC5 is heavily phosphorylated within established functional domains of the protein[26]. Despite the number of sites within the protein now known to be modified by phosphorylation, understanding of the functional roles and regulation of these HDAC5 phosphorylations remains limited (Figure 1A). As indicated above, the only HDAC5 phosphorylation sites that are functionally characterized are the two

sites on either side of the NLS that are critical for nucleo-cytoplasmic shuttling [18, 22, 23], and the two sites within the NLS that are important for nuclear import and cell cycle regulation [26, 29]. However, the sites within the other HDAC5 domains, AD, DAC, and NES, have not been yet characterized. Interestingly, while previously characterized phosphorylations of HDAC5 demonstrated high degrees of conservation in other class IIa HDACs, examination of sequence conservation among class IIa HDACs for the AD, DAC, and NES sites demonstrated that these sites are specific to HDAC5 (Figure 1B). Furthermore, these sites appear to be highly conserved among mammalian orthologues of HDAC5. Thus, these sites may represent distinct regulatory features of HDAC5. Therefore, we first assessed the abundance of these HDAC5 phosphorylations by mass spectrometry. As phosphorylations tend to be transient events, it is likely that individual phosphorylated forms of these residues are minority species. Moreover, certain phosphorylation events may have tight temporal regulations and would not be readily observed in an asynchronous population of cells, as is the case with phosphorylation of Ser278 [29]. To measure approximate phosphorylation levels, we calculated the ratios of peak areas for phosphorylated peptides and their unmodified counterparts for pSer611, pSer755, and pSer1108 using Skyline. We observed prominent phosphorylation of Ser611, ranging between 10 and 50%, and of Ser1108, ranging from 25 to 80%, while Ser755 phosphorylation was less readily observed, at ~3% (Figure 1C). Since phosphorylation usually leads to decreased peptide ionization efficiency, these are likely underestimates of phosphorylation levels. Given the likely dynamic nature of phosphorylation events, as well as the dynamic localization and temporal regulation of HDAC5, it is not surprising that phosphorylation abundances span a broad range of values. While this result highlights a common challenge in studies probing the effects of individual sites of post-translational modification, it also points to Ser611 and Ser1108 as sites prominently modified. Therefore, these sites could contribute structurally to the conformation of HDAC5 or may be required for important protein interactions. To investigate this aspect, we next assessed the location of these phosphorylations within the HDAC5 structure. While the structure of HDAC5 remains unsolved, structural predictions based on solved structures of other HDACs (i.e., HDAC4 [43]) were generated using the I-TASSER algorithm (Figure 1D). The depicted colors indicate functional HDAC5 domains in Figure 1A. Phosphorylations appear to map throughout the protein structure, both to the external face of the C-shaped structure, as well as to the inner surface (Figure 1D, **pink spheres**). Interestingly, the three phosphorylations discussed in this study, Ser611 (AD), Ser755 (DAC), and Ser1108 (NES) are predicted to map to the external edge of the protein, indicating that these sites may modulate HDAC5 protein interactions.

Site-specific phosphorylation impact HDAC5 protein interactions

To investigate the effect of phosphorylation on HDAC5 localization and interactions, we generated a series cell lines stably expressing phosphomutant HDAC5-EGFP. Site-specific serine-to-alanine mutations(S611A, S755A, and S1108A) rendered these HDAC5 variants phosphorylation incompetent within the targeted domains. We first assessed whether these HDAC5 phosphomutants exhibited altered cellular localization. Confocal microscopy with antibodies against GFP demonstrated that the phosphomutants exhibited dual nuclear and cytoplasmic localizations, similar to the wild-type HDAC5 (Figure 2A). We could confirm

this dual localization using direct fluorescence (Supplementary Figure S1), indicating that this is not an artifact of staining with the anti-GFP antibodies. Therefore, the lack of phosphorylation at these sites does not significantly impede HDAC5 shuttling. It remains to be established if a subset of HDAC5 has altered localizations within these subcellular compartments (i.e., within the nucleus or cytoplasm).

To assess phosphorylation-dependent protein interactions, we isolated EGFP-tagged wild-type HDAC5 alongside parallel isolations of the three domain phosphomutants using immunoaffinity purifications via the GFP tags (Figure 2B). Parallel immunoaffinity purification of EGFP from cells expressing EGFP alone served as controls for non-specific associations to the tag, magnetic beads, and antibody. We have previously optimized this method to efficiently recover HDAC5 with its known interactions [29]and have previously reported interactions for wild-type HDAC5 in CEM T cells[14]. Following immunoisolations, HDAC5 and its protein interactions were identified by mass spectrometry analyses. As expected, these proteins included well-established direct and indirect HDAC5 interactions, such as the nuclear co-repressor complex (NCOR1, NCOR2, TBL1X, TBL1XR1, GPS2), the MEF2 transcription factors, and the 14–3–3 chaperones required for HDAC5 nuclear export (Figure 3). Comparisons of individual protein spectrum counts allowed for label-free quantification of changes in the abundances of interacting proteins upon phosphomutation of individual residues. To assess the global impact of phosphomutation on HDAC5 interactions, we first examined the overall distribution of fold changes in protein abundances in each mutant (AD, DAC, and NES) isolation. The majority of interactions remained relatively unchanged (−1 to +1, log_2 scale) (Figure 2C). This result is consistent with the hypothesis that these phosphorylations may mediate specific protein interactions, but likely would not be sufficient to drastically disrupt the global HDAC5 interaction space. The proteins lying at either the positive or negative extremes of these distributions are likely good candidates for phosphorylation-dependent interactions.

To more specifically examine altered protein interactions, we assessed the specificity of interaction using the SAINT algorithm [36]. For these analyses, we used the protein interaction datasets obtained from our multiple biological replicates (n=3 for phosphomutants and HDAC5-EGFP, and n=4 for GFP controls). The majority of known HDAC5 interactions were observed in these isolations, passing the stringent SAINT specificity threshold of 0.90. Altogether, 94 proteins passed the SAINT filter and were identified as likely specific interactions of HDAC5. While this strategy provides an unbiased filtration of interactions and increased confidence in interaction specificity, one caveat of this approach is that the SAINT algorithm may under-represent specificity scores for low abundance or transient interactions of bait proteins, as we have previously observed for this class of enzymes[14]. As HDAC5 and the other class IIa HDACs shuttle between the nucleus and the cytoplasm, five well-established interacting partners did not pass the stringent SAINT specificity threshold of 0.90. Therefore, the transcription factors MEF2C and MEF2D, the kinases Aurora B and CaMK2D, and the phosphatase $PP2A_{cs}$, which were identified in our isolations but with fewer spectral counts and therefore lower SAINT scores, were added manually to the protein lists. It is not surprising that these proteins have lower spectral counts in asynchronous cells, as the association with Aurora B is cell cycle-

dependent and MEF2C and MEF2D are temporally regulated during development[29, 44]. We integrated information from the STRING database with our datasets to build protein interaction networks for each of the phosphorylation mutants. Protein abundances were mapped to these networks to identify proteins and protein complexes that change in association with HDAC5. Fold changes are represented as log_2 ratios of normalized spectrum counts for mutant and wild-type HDAC5 isolations (Figure 3). Interestingly, a range of interaction changes were observed for the various phosphomutants.

Globally, we observed a decrease in interactions for the AD and NES mutants (Figure 3A and B). These interaction changes were consistent among biological replicates (Supplemental Figure S2). Moreover, the global losses in interactions are in agreement with the observed greater abundances of phosphorylation at these sites and could indicate that HDAC5 must be phosphorylated at these sites to maintain a substantial portion of its interactions. This observation is consistent with the hypothesis that the AD and NES phosphorylations are important for maintaining functional conformation and protein structure. A general loss in association with the nuclear co-repressor complex as a whole (NCOR1, NCOR2, TBL1X, TBL1XR1, GPS2) was observed upon AD or NES mutation. This was accompanied by a slight increase in associations with the 14–3–3 chaperone proteins, which was more prominent for the NES mutant. The mechanism of HDAC nuclear export is not yet fully understood, but thought to involve a conformational change exposing the NES[18]. Given the observed changes in interactions, this NES phosphorylation may contribute to the conformational rearrangement.

While the DAC mutant had overall an increase in interactions, we also observed an increase in variability of the interactions from one biological replicate to the other (Supplemental Figure S2). Therefore, we have higher confidence in interaction changes with higher fold differences. A notable increase in protein abundance was observed in a set of nucleolar proteins upon phosphomutation of the DAC domain (Figure 3C, *upper left*) that was not observed in the AD or NES mutants (Figure 3A and B). It is possible that the sub-nuclear localization of HDAC5 may be modulated by modification of this residue. Furthermore, proteins with roles in chromatin remodeling and transcription regulation were increased with this mutant, including BAZ1B and BAZ2A that we previously reported to interact with the class III deacetylase SIRT7[45]. Whether these protein associations might also be substrates for deacetylation by HDAC5 remains to be determined.

Phosphorylation within the acidic domain modulates interactions with MEF2D, NCOR1, TBL1X, and HDAC3

To further examine modulation of protein associations mediated by phosphorylation within these functional domains, we validated a subset of HDAC5 protein interactions related to transcriptional repressive functions. While our study revealed both known and previously uncharacterized HDAC5 protein associations, we elected to focus on understanding the impact of phosphorylation on interactions known to becritical for the transcriptional repressive function of HDAC5, such as members of the nuclear co-repressor complex (NCOR1 and TBL1X) and the transcription factor MEF2D. In our label-free mass spectrometry approach, both AD and NES mutants displayed decreased associations with

components of the nuclear co-repressor complex. Interestingly, their association with HDAC3, a class I enzyme important for the *in vivo* deacetylation activity of HDAC5, was differentially modulated (Figure 3A and B, *upper left quadrant*). To validate these findings, small-scale immunoaffinity purifications of AD and NES phosphomutants and wild-type HDAC5 were performed for Western blotting analyses. These experiments recapitulated the changes in protein association observed by mass spectrometry-based label-free quantification. Both the AD and NES mutants exhibited a loss in association with the NCoR complex component TBL1X, while HDAC3 association appears increased upon AD mutation and decreased upon NES mutation (Figure 4Aand B). HDAC3 interaction with HDAC5 is understood to occur through bridging associations of NCoR complex associations; however, it is possible that HDAC5 interacts with HDAC3 as part of additional protein complexes and independently of other NCoR members.

To further confirm some of the observed changes in associations with proteins for which antibodies are less reliable, we next designed a parallel reaction monitoring (PRM) approach for targeted mass spectrometry quantification. We first used this approach to confirm the decrease in association with NCOR1 by selecting two NCOR1 peptides for fragmentation. Peak area integration allowed for quantification of peptide abundance as a proxy for protein abundance within immunoisolates. To exclude the possibility that abundance changes could be due to variation in bait isolation, we selected HDAC5 peptides for fragmentation and used the resulting peak areas for normalization against the bait. The PRM analysis confirmed the decrease in association of the AD mutant with NCOR1 in this additional biological replicate (Figure 4C, *right*). HDAC5-associated transcriptional repression within the nucleus is also closely linked to MEF2D expression and transcription factor binding is thought to promote association of HDAC-corepressor complexes with genomic regions. Therefore, we next investigated the observed increase in MEF2D association upon loss of AD phosphorylation (Figure 3A). PRM analysis of MEF2D peptides demonstrated a two-fold increase in association of MEF2D with HDAC5 (Figure 4C). Thus, it appears that phosphorylation of AD and NES sites impacts the association of HDAC5 with binding partners important in transcriptional regulation. We previously noted that the mutation of the NES or AD sites did not have a significant impact on the ability of the enzyme to deacetylase substrates *in vitro*[26]; therefore, the *in vivo* regulatory effects of these phosphorylations are more likely acting through modulation of protein associations and targeting HDAC5 to specific substrates rather than having a direct effect on the enzymatic activity of its DAC domain.

4. Concluding Remarks

In the past decade, phosphorylation has been established as an important regulator of protein function in health and disease systems. As the sensitivity of mass spectrometry instrumentation and methods for enriching and identifying phosphorylations have significantly improved, it has become apparent that a large percentage of proteins are phosphorylated. Global and targeted phosphorylation studies have led to the identification of numerous phosphorylations modifying proteins important for diverse cellular functions. The challenge now is to understand the function of these individual phosphorylations. From numerous previous studies, it is evident that phosphorylations can contribute to protein

activity and structure, as well as to the formation or disruption of interactions(e.g., [26, 29, 46–49]). Nevertheless, there is also the possibility of random events that can lead to phosphorylations without concrete functions. From an evolutionary perspective, this plasticity confers some benefits, and it may not be advantageous to inhibit a phosphorylation event that does not impact protein function. The challenge of studying the function of a specific phosphorylation is further amplified by the fact that phosphorylations are both spatially and temporally dynamic, and therefore, capturing the precise biologically relevant moment is not always straightforward.

In the context of class IIa HDACs, phosphorylation is known to regulate the transcriptional repressive functions of these enzymes by altering their subcellular localizations. The phosphorylations that have been reported to modulate HDAC5 protein localization are well conserved across the class IIa subfamily; however, additional HDAC5-specific phosphorylations that are well-conserved across divergent species may point to promising candidates for the investigation of unique HDAC5 functions. Here, we have examined well-conserved HDAC5 phosphorylations within its AD, DAC, and NES functional domains. Interestingly, we observed prominent phosphorylation of HDAC5 within the AD and NES domains, suggesting either a contribution to structural stability or the formation of protein interactions. Conversely, the low abundance of Ser755 phosphorylation within the DAC domain may indicate that this modification is important for interaction with specific substrates, or that this site has tight spatial or temporal regulation. Using immunoaffinity purification and mass spectrometry approaches, we constructed HDAC5 interaction networks for AD, DAC, and NES phosphomutants and identified differential modulation of specific protein interactions. We observed a global decrease in protein interactions upon mutation of the AD and NES, accompanied by specific loss of association with components of the NCoR complex important for transcriptional repression. Interestingly, we observed increased association of HDAC5 with HDAC3 and MEF2D upon loss of phosphorylation within the AD domain. Altogether, this study supports the model in which HDAC5 protein associations and functions are closely and carefully regulated by its phosphorylation status, and that investigation of site-specific phosphomutants within functional domains provides an important platform for defining and identifying novel regulatory roles of HDACs in human cells.

Supplementary Material

Refer to Web version on PubMed Central for supplementary material.

Acknowledgments

We are grateful to T. M. Greco for assistance in designing PRM analyses and to J. Chen for assistance with cell line validation. We thank G. Laevsky (Confocal Microscopy Core Facility, Princeton University) and C. DeCoste (Flow Cytometry Core Facility, Princeton University) for technical support. This work was supported by NIH grants DP1DA026192, R21AI102187, and R21HD073044 to IMC, an NSF graduate fellowship to AJG, and a National Health & Medical Research Council of Australia Early Career CJ Martin Fellowship APP1037043 to RAM.

Abbreviations

ABC	ammonium bicarbonate
ACN	acetonitrile
AD	acidic domain
Cdk5	cyclin-dependent kinase 5
DAC	deacetylation domain
DAPI	4′,6-diamidino-2-phenylindole
DPBS	Dulbecco's phosphate buffered saline
HDAC	histonedeacetylase
HEK293	human embryonic kidney cells
NCoR	the nuclear corepressor complex
NES	nuclear export sequence
NLS	nuclear localization signal
MEF2D	myocyte enhancer factor 2D
PKA	protein kinase A
PRM	parallel reaction monitoring
PVDF	polyvinylidine fluoride
RCSB PDB	Research Collaboratory for Structural Bioinformatics Protein Data Bank
SAINT	Significance Analysis of Interactome computational tool
WT	wild type

References

1. Inoue A, Fujimoto D. ENZYMATIC DEACETYLATION OF HISTONE. Biochemical and Biophysical Research Communications. 1969; 36:146. [PubMed: 5796748]
2. Berger SL. The complex language of chromatin regulation during transcription. Nature. 2007; 447:407–412. [PubMed: 17522673]
3. Renthal W, Maze I, Krishnan V, Covington HE 3rd, et al. Histone deacetylase 5 epigenetically controls behavioral adaptations to chronic emotional stimuli. Neuron. 2007; 56:517–529. [PubMed: 17988634]
4. Bossuyt J, Helmstadter K, Wu X, Clements-Jewery H, et al. Ca2+/Calmodulin-Dependent protein kinase II delta and protein kinase D overexpression reinforce the histone deacetylase 5 redistribution in heart failure. Circulation Research. 2008; 102:695–702. [PubMed: 18218981]
5. Yang XJ, Seto E. The Rpd3/Hda1 family of lysine deacetylases: from bacteria and yeast to mice and men. Nat Rev Mol Cell Biol. 2008; 9:206–218. [PubMed: 18292778]
6. Guise AJ, Budayeva HG, Diner BA, Cristea IM. Histone Deacetylases in Herpesvirus Replication and Virus-Stimulated Host Defense. Viruses-Basel. 2013; 5:1607–1632.
7. Murphy JC, Fischle W, Verdin E, Sinclair JH. Control of cytomegalovirus lytic gene expression by histone acetylation. Embo J. 2002; 21:1112–1120. [PubMed: 11867539]
8. Yang XJ, Gregoire S. Class II histone deacetylases: from sequence to function, regulation, and clinical implication. Molecular and Cellular Biology. 2005; 25:2873–2884. [PubMed: 15798178]

9. Archin NM, Keedy KS, Espeseth A, Dang H, et al. Expression of latent human immunodeficiency type 1 is induced by novel and selective histone deacetylase inhibitors. Aids. 2009; 23:1799–1806. [PubMed: 19590405]
10. Poon APW, Liang Y, Roizman B. Herpes simplex virus 1 gene expression is accelerated by inhibitors of histone deacetylases in rabbit skin cells infected with a mutant carrying a cDNA copy of the infected-cell protein no. 0. J Virol. 2003; 77:12671–12678. [PubMed: 14610189]
11. Huynh KD, Fischle W, Verdin E, Bardwell VJ. BCoR, a novel corepressor involved in BCL-6 repression. Genes & Development. 2000; 14:1810–1823. [PubMed: 10898795]
12. Takami Y, Nakayama T. N-terminal region, C-terminal region, nuclear export signal, and deacetylation activity of histone deacetylase-3 are essential for the viability of the DT40 chicken B cell line. Journal of Biological Chemistry. 2000; 275:16191–16201. [PubMed: 10748092]
13. Fischle W, Dequiedt F, Hendzel MJ, Guenther MG, et al. Enzymatic activity associated with class II HDACs is dependent on a multiprotein complex containing HDAC3 and SMRT/N-CoR. Molecular cell. 2002; 9:45–57. [PubMed: 11804585]
14. Joshi P, Greco TM, Guise AJ, Luo Y, et al. The functional interactome landscape of the human histone deacetylase family. Molecular Systems Biology. 2013:9.
15. Chang S, McKinsey TA, Zhang CL, Richardson JA, et al. Histone deacetylases 5 and 9 govern responsiveness of the heart to a subset of stress signals and play redundant roles in heart development. Molecular and cellular biology. 2004; 24:8467–8476. [PubMed: 15367668]
16. Vega RB, Harrison BC, Meadows E, Roberts CR, et al. Protein kinases C and D mediate agonist-dependent cardiac hypertrophy through nuclear export of histone deacetylase 5. Molecular and cellular biology. 2004; 24:8374–8385. [PubMed: 15367659]
17. Zhou X, Richon VM, Rifkind RA, Marks PA. Identification of a transcriptional repressor related to the noncatalytic domain of histone deacetylases 4 and 5. Proceedings of the National Academy of Sciences of the United States of America. 2000; 97:1056–1061. [PubMed: 10655483]
18. McKinsey TA, Zhang CL, Olson EN. Identification of a signal-responsive nuclear export sequence in class II histone deacetylases. Molecular and cellular biology. 2001; 21:6312–6321. [PubMed: 11509672]
19. Miska EA, Karlsson C, Langley E, Nielsen SJ, et al. HDAC4 deacetylase associates with and represses the MEF2 transcription factor. Embo J. 1999; 18:5099–5107. [PubMed: 10487761]
20. Grozinger CM, Schreiber SL. Regulation of histone deacetylase 4 and 5 and transcriptional activity by 14–3–3-dependent cellular localization. Proceedings of the National Academy of Sciences of the United States of America. 2000; 97:7835–7840. [PubMed: 10869435]
21. Wang AH, Kruhlak MJ, Wu J, Bertos NR, et al. Regulation of histone deacetylase 4 by binding of 14–3–3 proteins. Molecular and Cellular Biology. 2000; 20:6904–6912. [PubMed: 10958686]
22. Kao HY, Verdel A, Tsai CC, Simon C, et al. Mechanism for nucleocytoplasmic shuttling of histone deacetylase 7. Journal of Biological Chemistry. 2001; 276:47496–47507. [PubMed: 11585834]
23. McKinsey TA, Zhang CL, Lu J, Olson EN. Signal-dependent nuclear export of a histone deacetylase regulates muscle differentiation. Nature. 2000; 408:106–111. [PubMed: 11081517]
24. Gregoretti IV, Lee YM, Goodson HV. Molecular evolution of the histone deacetylase family: Functional implications of phylogenetic analysis. Journal of Molecular Biology. 2004; 338:17–31. [PubMed: 15050820]
25. Hubbert C, Guardiola A, Shao R, Kawaguchi Y, et al. HDAC6 is a microtubule-associated deacetylase. Nature. 2002; 417:455–458. [PubMed: 12024216]
26. Greco TM, Yu F, Guise AJ, Cristea IM. Nuclear Import of Histone Deacetylase 5 by Requisite Nuclear Localization Signal Phosphorylation. Molecular & Cellular Proteomics. 2011:10.
27. Ha CH, Kim JY, Zhao JJ, Wang WY, et al. PKA phosphorylates histone deacetylase 5 and prevents its nuclear export, leading to the inhibition of gene transcription and cardiomyocyte hypertrophy. Proceedings of the National Academy of Sciences of the United States of America. 2010; 107:15467–15472. [PubMed: 20716686]
28. Taniguchi M, Carreira MB, Smith LN, Zirlin BC, et al. Histone Deacetylase 5 Limits Cocaine Reward through cAMP-Induced Nuclear Import. Neuron. 2012; 73:108–120. [PubMed: 22243750]

29. Guise AJ, Greco TM, Zhang IY, Yu F, Cristea IM. Aurora B-dependent Regulation of Class IIa Histone Deacetylases by Mitotic Nuclear Localization Signal Phosphorylation. Molecular & Cellular Proteomics. 2012; 11:1220–1229. [PubMed: 22865920]
30. Cristea IM, Chait BT. Affinity purification of protein complexes. Cold Spring Harbor protocols. 2011; 2011
31. Rappsilber J, Mann M, Ishihama Y. Protocol for micro-purification, enrichment, pre-fractionation and storage of peptides for proteomics using StageTips. Nature Protocols. 2007; 2:1896–1906.
32. Elias JE, Gygi SP. Target-decoy search strategy for increased confidence in large-scale protein identifications by mass spectrometry. Nature Methods. 2007; 4:207–214. [PubMed: 17327847]
33. Olsen JV, de Godoy LMF, Li GQ, Macek B, et al. Parts per million mass accuracy on an orbitrap mass spectrometer via lock mass injection into a C-trap. Molecular & Cellular Proteomics. 2005; 4:2010–2021. [PubMed: 16249172]
34. Keller A, Nesvizhskii AI, Kolker E, Aebersold R. Empirical statistical model to estimate the accuracy of peptide identifications made by MS/MS and database search. Analytical chemistry. 2002; 74:5383. [PubMed: 12403597]
35. Kall L, Canterbury JD, Weston J, Noble WS, MacCoss MJ. Semi-supervised learning for peptide identification from shotgun proteomics datasets. Nature Methods. 2007; 4:923–925. [PubMed: 17952086]
36. Choi H, Larsen B, Lin ZY, Breitkreutz A, et al. SAINT: probabilistic scoring of affinity purification-mass spectrometry data. Nature Methods. 2011; 8:70–U100. [PubMed: 21131968]
37. Jensen LJ, Kuhn M, Stark M, Chaffron S, et al. STRING 8-a global view on proteins and their functional interactions in 630 organisms. Nucleic Acids Research. 2009; 37:D412–D416. [PubMed: 18940858]
38. Cline MS, Smoot M, Cerami E, Kuchinsky A, et al. Integration of biological networks and gene expression data using Cytoscape. Nature Protocols. 2007; 2:2366–2382.
39. MacLean B, Tomazela DM, Shulman N, Chambers M, et al. Skyline: an open source document editor for creating and analyzing targeted proteomics experiments. Bioinformatics. 2010; 26:966–968. [PubMed: 20147306]
40. Zhang Y. I-TASSER server for protein 3D structure prediction. Bmc Bioinformatics. 2008; 9
41. Roy A, Kucukural A, Zhang Y. I-TASSER: a unified platform for automated protein structure and function prediction. Nature Protocols. 2010; 5:725–738.
42. Roy A, Yang J, Zhang Y. COFACTOR: an accurate comparative algorithm for structure-based protein function annotation. Nucleic Acids Research. 2012; 40:W471–W477. [PubMed: 22570420]
43. Bottomley MJ, Lo Surdo P, Di Giovine P, Cirillo A, et al. Structural and functional analysis of the human HDAC4 catalytic domain reveals a regulatory structural zinc-binding domain. The Journal of biological chemistry. 2008; 283:26694–26704. [PubMed: 18614528]
44. Black BL, Olson EN. Transcriptional control of muscle development by myocyte enhancer factor-2 (MEF2) proteins. Annual Review of Cell and Developmental Biology. 1998; 14:167–196.
45. Tsai Y-C, Greco TM, Boonmee A, Miteva Y, Cristea IM. Functional Proteomics Establishes the Interaction of SIRT7 with Chromatin Remodeling Complexes and Expands Its Role in Regulation of RNA Polymerase I Transcription. Molecular & Cellular Proteomics. 2012; 11
46. Holt LJ, Tuch BB, Villen J, Johnson AD, et al. Global Analysis of Cdk1 Substrate Phosphorylation Sites Provides Insights into Evolution. Science. 2009; 325:1682–1686. [PubMed: 19779198]
47. Huttlin EL, Jedrychowski MP, Elias JE, Goswami T, et al. A Tissue-Specific Atlas of Mouse Protein Phosphorylation and Expression. Cell. 2010; 143:1174–1189. [PubMed: 21183079]
48. Melo-Braga MN, Schulz M, Liu Q, Swistowski A, et al. Comprehensive Quantitative Comparison of the Membrane Proteome, Phosphoproteome, and Sialiome of Human Embryonic and Neural Stem Cells. Molecular & Cellular Proteomics. 2014; 13:311–328. [PubMed: 24173317]
49. Klimovskaia IM, Young C, Stromme CB, Menard P, et al. Tousled-like kinases phosphorylate Asf1 to promote histone supply during DNA replication. Nature communications. 2014; 5:3394–3394.

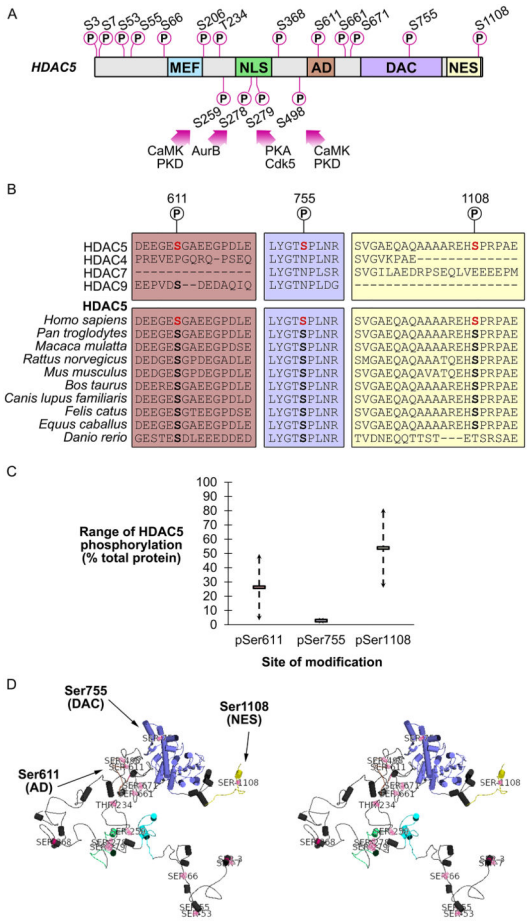

Figure 1. HDAC5 is phosphorylated within functional domains

(A) HDAC5 domains and site localization of individual phosphorylation. Functionally characterized phosphorylation sites and corresponding kinases are displayed on the bottom of the protein schematic, whereas yet-uncharacterized sites appear on the top of the schematic. MEF2, MEF2-binding domain; NLS, nuclear localization signal; AD, acidic domain; DAC, deacetylation domain; NES, nuclear export sequence. (B) HDAC5 sequence alignment with class IIa HDACs (HDAC4, 7, and 9) and mammalian orthologues for AD, DAC, and NES domain phosphorylations. (C) Mean percentage of total HDAC5 protein phosphorylated at individual sites calculated from phosphopeptide peak areas. Error bars represent standard deviation (pSer611 and pSer755, n=3; pSer1108, n=2). (D) Phosphorylations (pink spheres) mapped to a crystal structure prediction of HDAC5 generated using the I-TASSER modeling algorithm (Zhang Lab, University of Michigan).

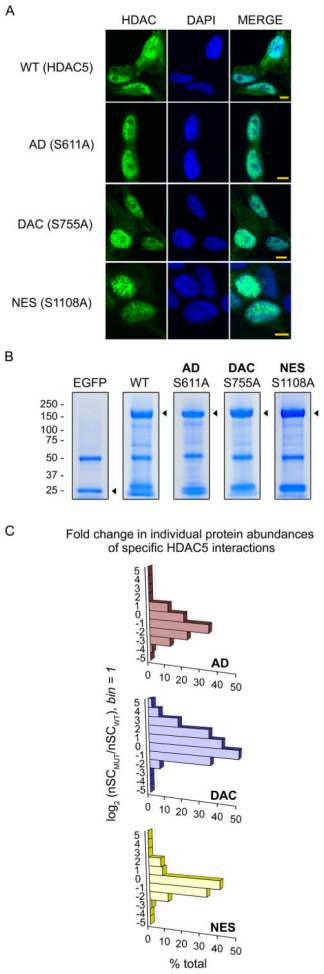

Figure 2. Characterization of HDAC5 domain phosphomutants

(A) Localization of wild-type and serine to alanine phosphomutant HDAC5-EGFP protein in HEK293 cells. Green: EGFP, HDAC5; blue: DAPI, nuclei; 100x oil immersion lens; scale bar = 10 μm. (B) Coommassie staining of immunoaffinity purified wild-type and phosphomutant HDAC5-EGFP (150 kDa) and control EGFP (27 kDa) resolved by SDS-PAGE. (C) Global distribution of individual fold changes of specific (SAINTp>0.90) HDAC5 protein interactions following immunoaffinity purification of phosphomutant and wild-type HDAC5-EGFP (n=3). Fold change was calculated as the log_2-transformed ratio of normalized spectrum counts (nSC) identified in mutant (MUT) and wild-type (WT) isolations.

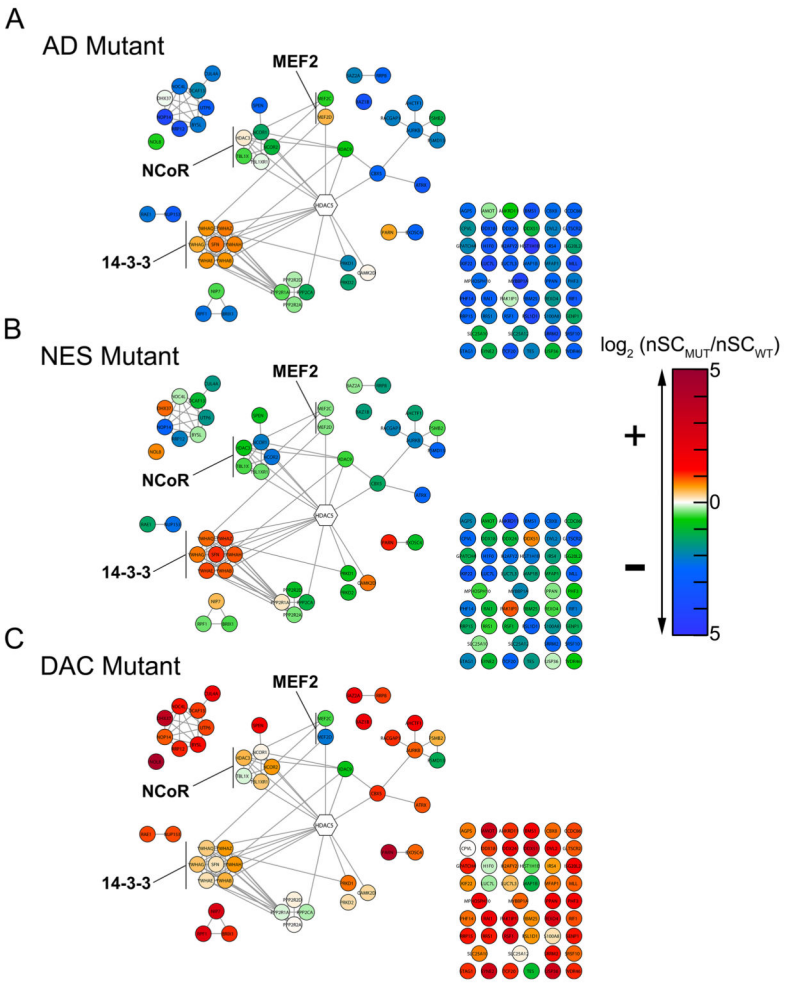

Figure 3. Building interaction networks for HDAC5 phosphomutants

Fold change in abundance of co-isolated proteins mapped to networks of specific HDAC5 protein interactions (SAINTp>0.90, n=3) calculated from ratios of normalized spectrum counts (log_2 nSC_{MUT}/nSC_{WT}). Networks were generated using STRING-db and Cytoscape. (A) Interaction map for the acidic domain (AD) mutant. (B) Interaction map for the nuclear export sequence (NES) domain mutant. (C) Interaction map for the deacetylation domain (DAC) mutant.

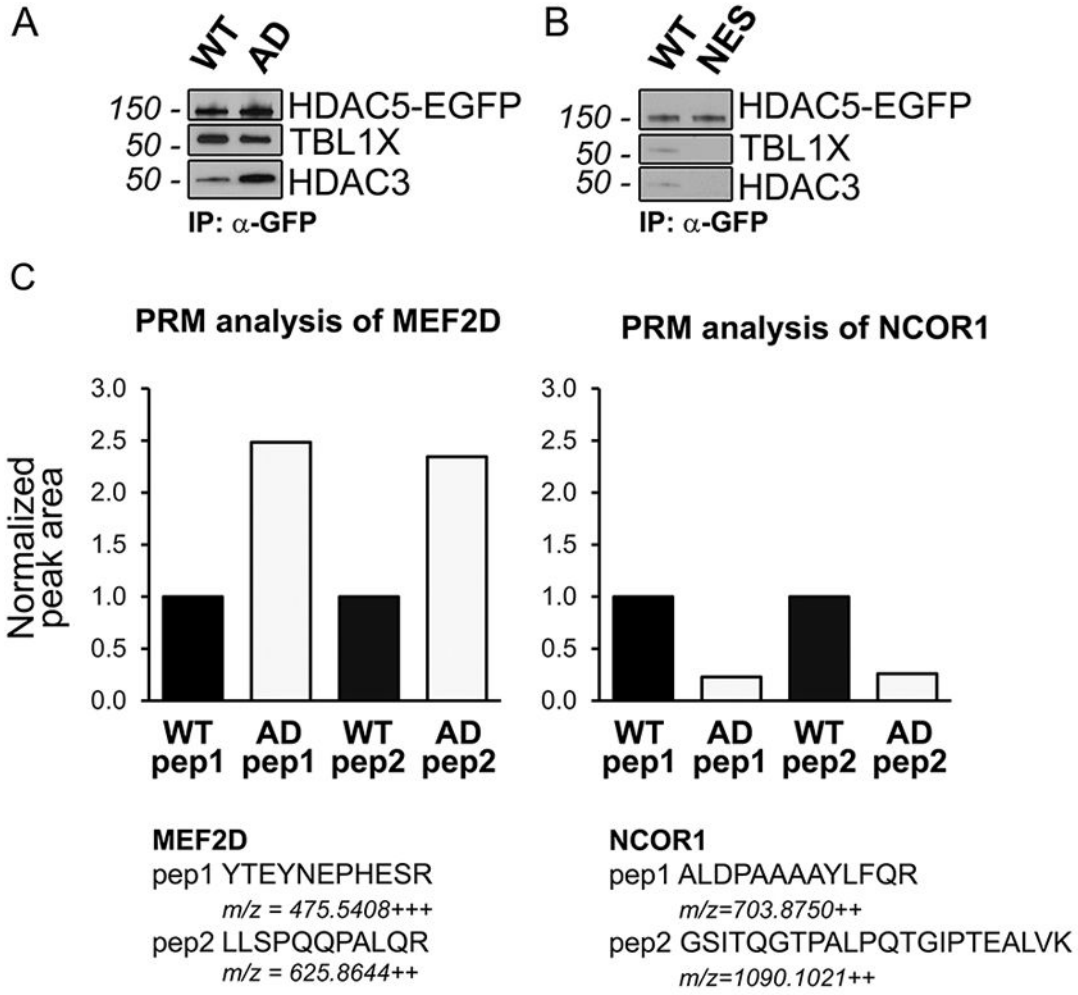

Figure 4. Validation of changes in protein interactions

(A, B) Co-isolation of HDAC3 and TBL1X with immunoaffinity purified wild-type and phosphomutant (AD and NES) HDAC5-EGFP identified by immunoblotting. (C) Quantitation of MEF2D and NCOR1 peptide peak areas using parallel reaction monitoring (PRM) LC-MS/MS analysis. Individual peptide peak areas (2 peptides per protein) were normalized to average HDAC5 bait peak areas (2 peptides per protein).